

Fatigue Crack Growth Resistance of Titanium Metal Matrix Composites

H. Stanley, M. Dear, T. J. A. Doel and P. Bowen

Abstract Fatigue crack growth resistance has been assessed in continuous SCS-6 fibre reinforced Ti-6Al-4V composites from unbridged defects at room temperature, 300 and 450 °C in air and in vacuum. The initial applied stress intensity factor range (ΔK_{app}) (on the unbridged crack depth) was used to quantify the crack arrest/catastrophic failure (CA/CF) transitions for all test conditions. All tests were conducted at stress ratios of 0.1, 0.5 and 0.7 and at a frequency of 4 Hz. Fatigue crack growth tests revealed that increased temperature results in increased fatigue crack growth rates. The CA/CF transition reduced as the temperature increased from room temperature to 300 °C and to 450 °C. The CA/CF transition of the composite is greatly affected by the initial ΔK_{app} value due to its effect on fibre failures. Crack bifurcation appears to be a function of test piece geometry and not a function of test temperature or the initial ΔK_{app} value. Tests in vacuum demonstrate that fatigue crack growth rates are reduced. All cracks in vacuum grew in single mode I. Longer fibre pull out lengths were observed in tests performed in vacuum compared with air for similar conditions, especially during 0.5 mm of growth from the notch. These fibres are deduced to bridge the crack for a long time, suggesting that the fibres in the first few rows are important to reduce crack growth rates and to promote crack arrest.

Keywords Fatigue crack growth · Titanium metal matrix composites
Temperature · Environmental effects · Crack arrest · Fibre pull out

H. Stanley (✉) · M. Dear · T. J. A. Doel · P. Bowen
School of Metallurgy and Materials, The University of Birmingham,
Edgbaston, Birmingham B15 2TT, UK
e-mail: hxs260@bham.ac.uk

© The Minerals, Metals & Materials Society 2018
T. S. Srivatsan et al. (eds.), *Metal-Matrix Composites Innovations, Advances and Applications*, The Minerals, Metals & Materials Series,
https://doi.org/10.1007/978-3-319-72853-7_7

Introduction

The constant need for increasing performance demands by aerospace systems calls for the development of new materials. Titanium metal matrix composites (Ti MMCs) reinforced with silicon carbide (SiC) fibres are of interest to the aerospace industry because of their high specific mechanical properties, especially specific strength and stiffness. They have the ability to decrease the weight of several key axi-symmetric components, and may allow radical changes in design, and thereby improve the overall efficiency of the engine. Previous studies have investigated their potential use within an aero engine, to replace monolithic alloys, but cost and complexities of the composite limit its use. Unlike its monolithic counterpart, Ti MMCs exhibit no unique relationship between the crack growth rates, da/dN , and the nominal applied stress intensity factor, ΔK_{app} [1–3]. Studies have shown that Ti MMCs exhibit fatigue crack growth resistance through the use of bridging fibres behind the crack tip. The bridging fibres resist the crack opening forces and can reduce the value of the crack-tip stress intensity range, ΔK_{tip} by providing crack closure forces, and can reduce fatigue crack growth rates with an increase in crack length, due to a greater number of fibres bridging the crack [1, 4–6]. If fibres remain intact, the propagating crack can arrest (CA), which is defined as $da/dN \leq 10^{-8}$ mm/cycle [7]. If some bridging fibres fracture the da/dN can increase, sometimes resulting in catastrophic failure (CF), therefore a transition between the two behaviours exists. This is known as the CA/CF transition and can be defined in terms of ΔK . This transition however is dependent on the number of bridging fibres in the crack wake as well as secondary factors such as the test temperature, environment, ΔK , and the stress ratio, R .

One possible area where Ti MMCs are being considered is in the compressor region of the engine where temperatures do not exceed 400 °C. One component that will benefit from the implementation of Ti MMCs is a bladed ring. By removing the need for the central bore the component will reduce its weight. This component will experience high stresses and cyclic loading and therefore Ti MMCs resistance to fatigue is of utmost importance. The circumferential fibres are able to support the hoop stress alone [7]. This paper attempts to characterise and discuss the fatigue crack growth resistance of a Ti-6Al-4V/SCS-6 composite at ambient and elevated temperatures, with particular attention to determining the CA/CF transitions. The effect of temperature, environment, and initial ΔK_{app} will be discussed, with some reference to pull out lengths and stress ratio.

Method

The Ti-6Al-4V/SCS-6 composite was of an 8-ply unidirectional layup with a fibre volume fraction of 35%. The precursor material was SCS-6 SiC fibre of 142 μm nominal diameter, incorporating a 3 μm carbon outer layer, with a Ti-6Al-4V

physical vapour deposition coating. The metal coated fibre was laid up as a panel in a hexagonal array, with a $\sim 150 \mu\text{m}$ cladding layer on either side. This was hot isostatic pressed to form the dense composite. Whilst the volume of the composite core was 35%, addition of the cladding layer reduced the overall volume fraction to $\sim 27\%$.

Test pieces of $75 \times 4 \times 1.9 \text{ mm}$ were cut for three point bend tests. A notch of 0.4 mm depth was cut into the middle of each test piece, perpendicular to the fibre direction using a $150 \mu\text{m}$ thick diamond blade, resulting in an initial crack depth to width ratio, a_0/W of 0.1.

The test pieces were loaded in three-point bend using a 60 mm span, giving a span to width ratio of 15:1. All tests were conducted using a servo-hydraulic machine operating in load control mode, using a 5kN range. The machine could be configured for testing at temperature and in air or vacuum as required. Load was applied using a sinusoidal waveform with maximum and minimum loads being at a constant level throughout each test. Tests were conducted at room temperature (20 °C), 300 and 450 °C, temperatures being monitored throughout using thermocouples attached to the test pieces.

Fatigue crack growth was monitored using the direct current potential difference (DCPD) technique. A constant current was applied to the test piece, and the resulting voltage across the notch was measured via spot welded platinum wires. As the crack length increased, the resistance increased, therefore according to the Ohm's Law, the voltage increased. A starting voltage of 1 mV was used across the notch and the V_0 value was adjusted in order to match the measured notch length with the calculated a_0 . The recorded voltage was used to calculate the crack length using the equation [8].

$$\frac{a}{W} = -0.45 + 0.954 \left(\frac{V}{V_0} \right) - 0.292 \left(\frac{V}{V_0} \right)^2 + 0.038 \left(\frac{V}{V_0} \right)^3$$

Stress ratio, R, values of 0.1, 0.5 and 0.7 and a frequency of 4 Hz was used. The tests performed at room temperature had initial ΔK_{app} values of between 18 and 30 $\text{MPa}\sqrt{\text{m}}$. Initial ΔK_{app} values between 14 and 23 $\text{MPa}\sqrt{\text{m}}$ were used for the test temperature of 300 °C. For tests conducted in air at 450 °C, initial ΔK_{app} values between 8 and 18 $\text{MPa}\sqrt{\text{m}}$ were used. Initial ΔK_{app} values between 15 and 30 $\text{MPa}\sqrt{\text{m}}$ were used to identify the effects that elevated temperature and environment has on fatigue crack growth resistance.

After each test the final crack length was measured from the fracture surface and checked against that given by the DCPD technique. The fracture faces were initially examined using low magnification optical images on a Leica stereo microscope, and they were then further examined using a Hitachi S4000 field emission gun scanning electron microscope (SEM) operating at 20 kV. All images were taken using the secondary electron detector. While examining the fracture faces, fibre pull out lengths were measured in the region of the mode I fatigue crack.

Results and Discussion

Fatigue Crack Growth Resistance

Due to the fibre bridging mechanism, it is not appropriate to present fatigue crack growth data as conventional da/dN versus nominal ΔK plots. The approach here is to compare the results in terms of da/dN versus crack length, a , for given values of the initial ΔK_{app} .

Note: The da/dN data in all figures and tables are stated for mode I crack lengths only. Bifurcation, where the crack can split and grow along the fibre/matrix interface, is observed in some tests within this paper. Bifurcation invalidates the DCPD calibration curve and hence data is shown only to the bifurcation length.

Effects of ΔK at a Single Test Temperature

Figures 1, 3 and 4 display the fatigue crack growth curves for room temperature, 300 and 450 °C. The CA/CF transitions are shown in Table 1 for each temperature. From Fig. 1, at room temperature, the test at an initial ΔK_{app} value of 18 MPa \sqrt{m} reached crack arrest, where the effective ΔK reduced below matrix threshold levels. The test at an initial ΔK_{app} of 30 MPa \sqrt{m} experienced stable crack growth rates until rapid increases in da/dN were observed prior to catastrophic failure. The two tests performed at initial ΔK_{app} values of 21 and 23 MPa \sqrt{m} experienced very similar crack growth rates to the test that reached crack arrest but the fatigue crack

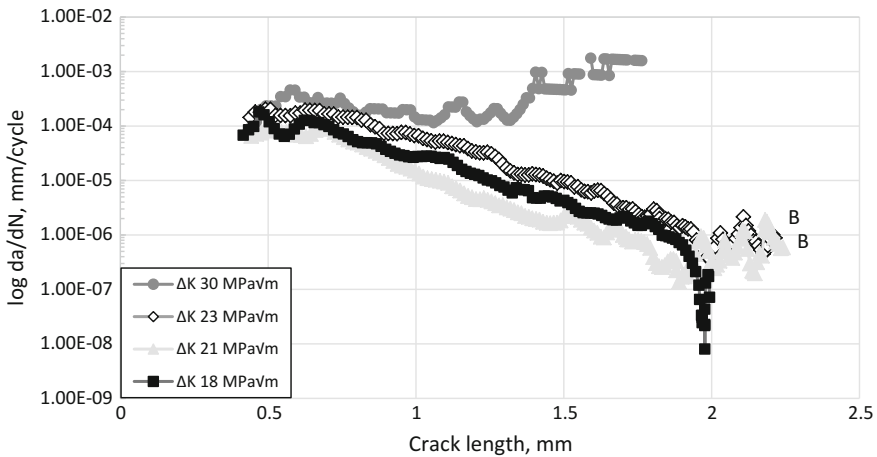


Fig. 1 Fatigue crack growth rate da/dN versus crack length for four different values of initial ΔK_{app} at $R = 0.1$ cycled at 4 Hz until failure or arrest at room temperature. *Note* The da/dN data for tests that bifurcated is only displayed up to the bifurcation crack length

Table 1 The initial ΔK_{app} values required for the CA/CF transition for each test temperature

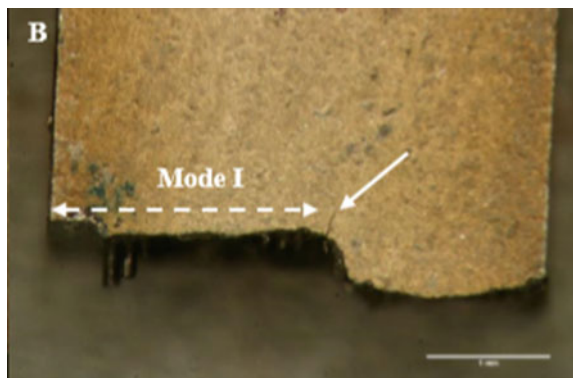
| Initial ΔK_{app} (MPa \sqrt{m}) | Temperature (°C) | Outcome |
|--|------------------|---------|
| 18 | 20 | Arrest |
| 21 | 20 | Failure |
| 14 | 300 | Arrest |
| 16 | 300 | Failure |
| 10 | 450 | Arrest |
| 12 | 450 | Failure |

in both of these eventually bifurcate at crack lengths of approximately 2.2 mm [9]. Therefore, the CA/CF transition at room temperature is estimated between 18 and 21 MPa \sqrt{m} . An image of bifurcation that occurred on the test at an initial ΔK_{app} of 21 MPa \sqrt{m} is shown in Fig. 2.

Figure 3 displays the results from the fatigue crack growth tests at 300 °C. The tests with at initial ΔK_{app} value of 18 MPa \sqrt{m} and below experienced periods of decreasing crack growth rates which almost led to crack arrest. Except for the test where crack arrest was actually achieved at an initial ΔK value of 14 MPa \sqrt{m} , the fatigue cracks bifurcated in each case. The test at an initial ΔK_{app} of 23 MPa \sqrt{m} experienced secondary cracking, where a second crack formed but it continued to grow in mode I direction until it bifurcated at a crack length of 2.25 mm.

The tests at 450 °C exhibited a similar trend to those at 300 °C, shown in Fig. 4. Tests performed at initial ΔK_{app} values of 8 and 10 MPa \sqrt{m} are deemed to have reached crack arrest, while for those tested at values greater than 12 MPa \sqrt{m} the fatigue crack bifurcated and the test piece failed. Therefore, the CA/CF transition is estimated between 10 and 12 MPa \sqrt{m} . The three tests where the crack bifurcated and failure occurred saw fatigue crack growth rates decrease after 0.55 mm of crack growth. At a ΔK_{app} of 18 MPa \sqrt{m} , da/dN continued to decrease at a stable rate until a crack length of 1.6 mm was reached, where the fatigue crack growth rates increased until final failure. For the tests performed at initial ΔK_{app} values of 12 and 16 MPa \sqrt{m} , da/dN was much less stable and a rapid increase in da/dN was observed near the failure crack length.

Fig. 2 Fractography of the test piece at an initial ΔK_{app} of 21 MPa \sqrt{m} . The dotted line indicates the mode I crack growth and the arrow points to the point of bifurcation [9]



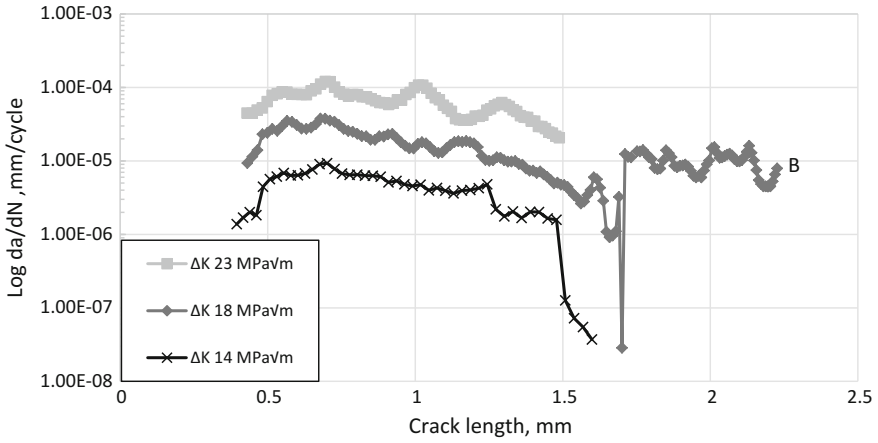


Fig. 3 Fatigue crack growth rate da/dN versus crack length for four different values of initial ΔK_{app} at $R = 0.1$ cycled at 4 Hz until failure or arrest at 300 °C. *Note* The da/dN data for tests that bifurcated is only displayed up to the bifurcation crack length. Data for initial ΔK_{app} 23 MPa $\sqrt{\text{m}}$ data is only displayed up to the length where a secondary crack formed

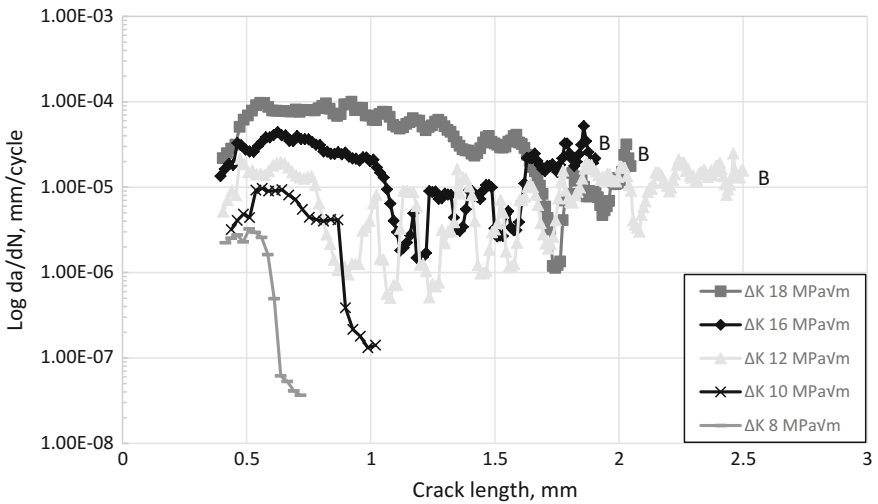


Fig. 4 Fatigue crack growth rate da/dN versus crack length for five different values of initial ΔK_{app} at $R = 0.1$ cycled at 4 Hz until failure or arrest at 450 °C. *Note* The da/dN data for tests that bifurcated is only displayed up to the bifurcation crack length

There is an initial increase in da/dN with increasing crack length. This occurs because the fatigue crack needs to grow approximately 0.25 mm from the notch to grow past one row of fibres and experience the effects of bridging fibres. After this initial increase the da/dN stabilises and starts to reduce. This reduction is an effect

Table 2 Number of cycles to arrest/failure for a number of tests across the three temperatures

| Condition | Crack length (mm) | Number of cycles to arrest/failure |
|--|-------------------|------------------------------------|
| 20 °C/ $\Delta K = 23 \text{ MPa}\sqrt{\text{m}}$ | 2.21 (B) | 1,285,448 579,288 (B) |
| 20 °C/ $\Delta K = 18 \text{ MPa}\sqrt{\text{m}}$ | 1.99 | 1,352,376 |
| 300 °C/ $\Delta K = 18 \text{ MPa}\sqrt{\text{m}}$ | 2.22 (B) | 260,265 214,296 (B) |
| 300 °C/ $\Delta K = 14 \text{ MPa}\sqrt{\text{m}}$ | 1.6 | 929,640 |
| 450 °C/ $\Delta K = 16 \text{ MPa}\sqrt{\text{m}}$ | 1.9 (B) | 203,400 186,660 (B) |
| 450 °C/ $\Delta K = 10 \text{ MPa}\sqrt{\text{m}}$ | 1.02 | 644,000 |

of the crack growing past fibres which are left bridging the crack wake. All fatigue crack growth results at room temperature, 300 and 450 °C indicate that a decrease in da/dN rates is observed with increasing crack length. For any given temperature, decreasing the initial ΔK_{app} increases the specimen lifetime (Table 2). Crack arrest is observed at the lowest values of initial ΔK_{app} used in this paper. The main mechanism promoting fatigue crack growth resistance is the presence of intact bridging fibres in the crack wake which shield the crack tip from the full effect of the ΔK_{app} [1]. The number and effect of these intact fibres in the crack wake is controlled by several factors; the fibre strength and distribution, the number of bridging fibres, the fibre matrix interfacial shear strength [10], the initial ΔK_{app} , manufacturing method and test temperature [3]. The sharp decreases in da/dN observed by all tests which arrest can be attributed to ΔK_{app} at the crack tip (ΔK_{tip}) falling below the threshold stress intensity range for the matrix, (ΔK_{th}). Bifurcation occurred in test pieces at each temperature at very similar crack lengths. This suggests bifurcation is not a function of test temperature or initial ΔK_{app} , but is a function of test piece geometry.

Effect of Temperature

Figure 5 shows the effect of test temperature on the fatigue crack growth rates at $R = 0.1$ in air and at an initial ΔK_{app} value of $18 \text{ MPa}\sqrt{\text{m}}$. The comparison of the curves suggest that the initial crack growth rates at all test temperatures are very similar. At a test temperature of 20 °C crack growth rates (da/dN) decreased until the crack arrested at a crack length of 1.99 mm. Increasing the test temperature to 300 and 450 °C increased the growth rates after 1.4 mm of crack growth until catastrophic failure was observed. Cracks in tests at 300 and 450 °C grew in mode I up to 2.22 and 2.04 mm respectively before bifurcating. The fatigue curves suggest that there is not much difference between test temperatures of 20 and 300 °C as the latter almost arrested at a crack length of 1.7 mm. This is confirmed by the similar crack growth rates at room temperature and 300 °C up to a crack length of 1.5 mm.

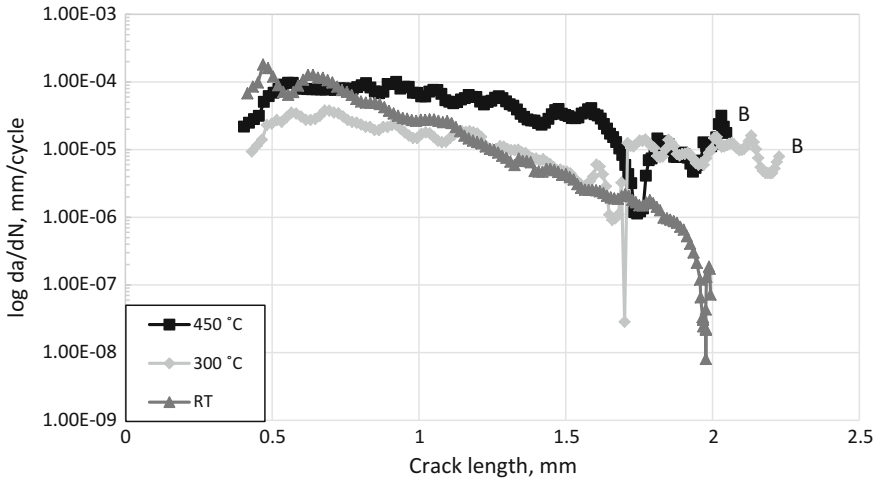


Fig. 5 Fatigue crack growth rate da/dN versus crack length for three different temperatures: 20, 300 and 450 °C. All tested at an initial ΔK_{app} of 18 MPa \sqrt{m} at $R = 0.1$ and 4 Hz. *Note* The da/dN data for tests that bifurcated is only displayed up to the bifurcation crack length

As the test temperature increased, the number of cycles to failure decreased and the final crack length increased (Table 3). Similar behaviour is also observed at $R = 0.5$ and 0.7 (Table 3), however the number of cycles to failure increased as the R ratio increased. It is difficult to find a CA/CF transition at higher R ratios at 450 °C as smaller initial ΔK_{app} values failed to initiate from the notch [11].

Table 1 shows that increasing the test temperature decreases the initial ΔK_{app} value at which the CA/CF transition occurs and increases the likelihood of bifurcation. There are multiple reasons why the fatigue crack growth resistance is greater at lower temperatures. Firstly, at elevated temperatures the matrix material itself may experience reduced fatigue crack growth resistance, increasing the fatigue crack growth rates of the composite [2]. Secondly, changes to the interfacial properties between the matrix and fibre during testing could arise from changes in the residual stresses or from effects of oxidation at the interface. The compressive stress exerted onto the fibres by the matrix is reduced at 450 °C due to the thermal expansion coefficient mismatch and therefore the likelihood of the fatigue crack propagating at the fibre/matrix interface is increased. If the interfacial strength decreases at higher temperatures, provided the fibre fracture strength stays the same, models based on ceramic matrix composites would suggest pull out lengths increase [12]. There is some indication of this from individual fibre tests and their interfacial properties, however as they are measured at room temperature and not at the operating temperatures, their results must be analysed with caution and an effective method of evaluating interfacial strengths at higher temperatures is needed. Pull out lengths for tests that reached crack arrest for each corresponding temperature are displayed in Table 4. There appears to be very little difference at all temperatures between average pull out lengths.

Table 3 Comparison of crack lengths and number of cycles for tests at different temperatures, environment conditions, R ratios and initial ΔK_{app} at a frequency of 4 Hz

| Temperature (°C) | Environment | R Ratio | Initial ΔK_{app} | | | | | | | | | | | | |
|---|-------------|---------|--------------------------|-------------------|------|---------|----|------|------|----|----|----|---|------|------|
| | | | 6 | 8 | 10 | 12 | 14 | 16 | 18 | 21 | 22 | 24 | | | |
| <i>Crack length (mm)</i> | | | | | | | | | | | | | | | |
| 20 | Air | 0.1 | - | - | - | - | - | - | - | - | - | - | - | - | - |
| 450 | Air | 0.1 | - | - | 1.02 | 2.5 (B) | - | - | - | - | - | - | - | - | - |
| 450 | Vacuum | 0.1 | - | - | - | - | - | - | - | - | - | - | - | 2.32 | 1.96 |
| 20 | Air | 0.5 | - | - | - | - | - | 1.37 | 2.22 | - | - | - | - | - | - |
| 450 | Air | 0.5 | - | 2.41 ^a | - | - | - | - | - | - | - | - | - | - | - |
| 20 | Air | 0.7 | - | - | - | 1.64 | - | 1.83 | - | - | - | - | - | - | - |
| 450 | Air | 0.7 | 2.36 ^a | - | - | - | - | - | - | - | - | - | - | - | - |
| <i>Number of cycles ($\times 100$)</i> | | | | | | | | | | | | | | | |
| 20 | Air | 0.1 | - | - | - | - | - | - | - | - | - | - | - | - | - |
| 450 | Air | 0.1 | - | - | 644 | 634 (B) | - | - | - | - | - | - | - | - | - |
| 450 | Vacuum | 0.1 | - | - | - | - | - | - | - | - | - | - | - | 1636 | 1000 |
| 20 | Air | 0.5 | - | - | - | - | - | 399 | 1708 | - | - | - | - | - | - |
| 450 | Air | 0.5 | - | 915 ^a | - | - | - | - | - | - | - | - | - | - | - |
| 20 | Air | 0.7 | - | - | - | 810 | - | 1277 | - | - | - | - | - | - | - |
| 450 | Air | 0.7 | 1575 ^a | - | - | - | - | - | - | - | - | - | - | - | - |

The two tests representing crack arrest and catastrophic failure have been displayed

^aCrack arrest did not occur and therefore the lowest initial ΔK value has been used

Note The data for tests that bifurcated is only displayed up to the bifurcation crack length and is denoted by ^(b)

Table 4 Showing the average fibre pull out length and maximum pull out length measured from one side of the fracture face on a SEM for three test temperatures

| Condition | Average pull out (mm) | S.D (mm) | Max pull out (mm) |
|--|-----------------------|----------|-------------------|
| 20 °C/ $\Delta K = 18 \text{ MPa}\sqrt{\text{m}}$ | 0.076 | 0.029 | 0.14 |
| 300 °C/ $\Delta K = 14 \text{ MPa}\sqrt{\text{m}}$ | 0.095 | 0.069 | 0.31 |
| 450 °C/ $\Delta K = 10 \text{ MPa}\sqrt{\text{m}}$ | 0.078 | 0.052 | 0.19 |

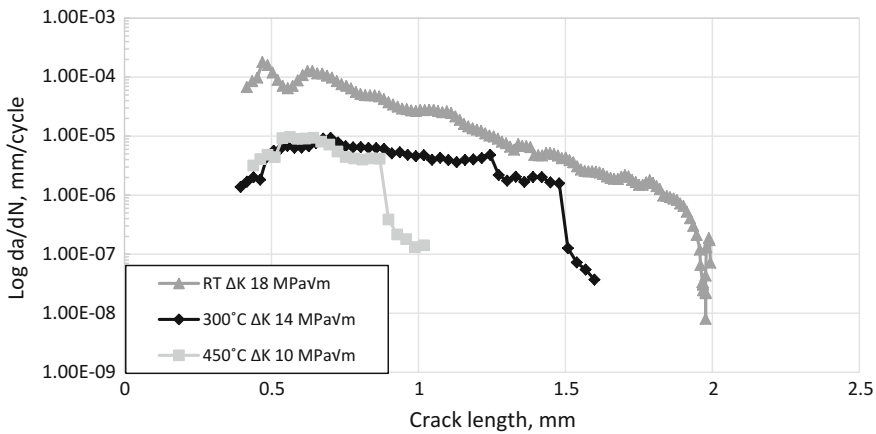


Fig. 6 Fatigue crack growth rate da/dN versus crack length for three different temperatures: 20, 300 and 450 °C and their corresponding crack arrest values of initial ΔK_{app} . $R = 0.1$ and 4 Hz

Figure 6 displays tests from the three temperatures and their corresponding crack arrest fatigue curves. Note the data displayed is data from the highest initial ΔK_{app} that arrested. It is clear that the maximum initial ΔK_{app} used to achieve crack arrest decreases progressively as the temperature is increased from room temperature to 300 and 450 °C.

Table 4 displays the average and maximum pull out lengths measured from the tests that arrested at the three temperatures. Despite the reduced residual stresses there appears to be no difference between room temperature and 450 °C. Figure 7 highlights the similarities of reduced pull out lengths at room temperature and 450 °C in air.

Effect of Environment (Air vs. Vacuum) at 450 °C

Testing in vacuum has a clear effect on fatigue crack growth rates when compared with tests in air and at room temperature (Fig. 8). The rates are much slower, by about two orders of magnitude in vacuum than tests performed in air at an $R = 0.1$ and similar initial ΔK_{app} values. Apart from the initial 0.1 mm of crack growth the

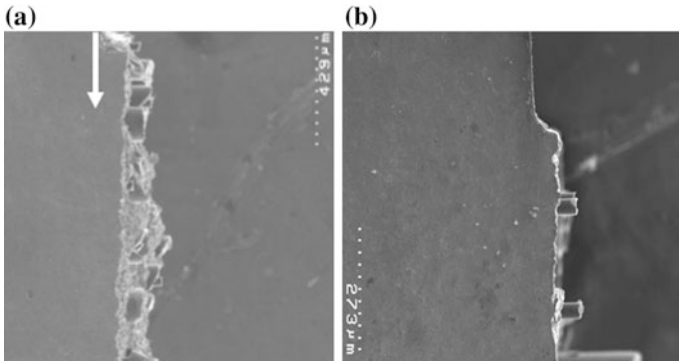


Fig. 7 SEM images showing the pull out lengths of the two tests performed at **a** Room temperature and an initial ΔK_{app} value of $18 \text{ MPa}\sqrt{\text{m}}$, and **b** $450 \text{ }^\circ\text{C}$ at an initial ΔK_{app} value of $10 \text{ MPa}\sqrt{\text{m}}$

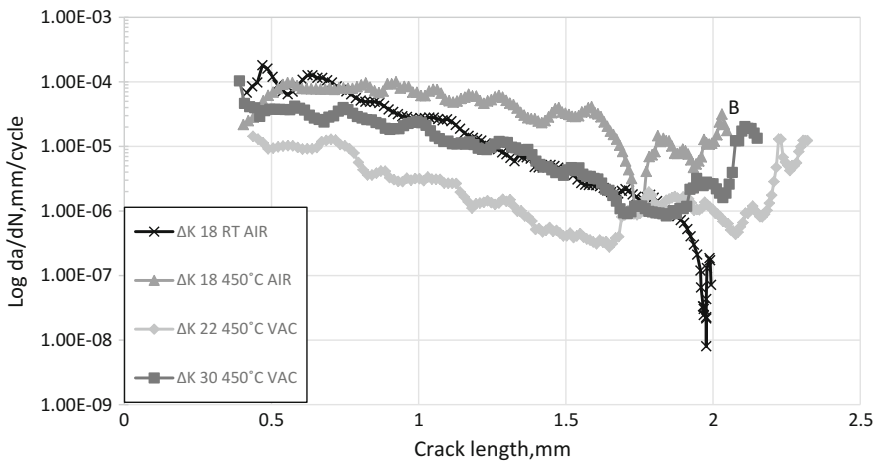


Fig. 8 Fatigue crack growth rate da/dN versus crack length for different values of initial ΔK_{app} at $R = 0.1$ cycled at 4 Hz until failure or arrest at room temperature and $450 \text{ }^\circ\text{C}$ in air and vacuum. *Note* The da/dN data for tests that bifurcated is only displayed up to the bifurcation crack length

test with an initial ΔK_{app} of $18 \text{ MPa}\sqrt{\text{m}}$ in air at $450 \text{ }^\circ\text{C}$ has higher crack growth rates than the test with an initial ΔK_{app} value of $30 \text{ MPa}\sqrt{\text{m}}$ in vacuum for the entirety of the test.

Although as of yet a CA/CF transition has not been established in vacuum at $450 \text{ }^\circ\text{C}$, the behaviour of the lowest initial ΔK_{app} value of $22 \text{ MPa}\sqrt{\text{m}}$ applied to date suggests that crack arrest will occur at a much higher initial ΔK_{app} value than air. It is obvious from the fatigue crack growth curves that for testing in vacuum decreases fatigue crack growth rates compared to air.

When comparing tests performed in vacuum at 450 °C and tests performed in air at room temperature the test with a much higher initial ΔK_{app} value of 30 MPa \sqrt{m} in vacuum has slightly reduced crack growth rates compared to that tested at room temperature which grows to crack arrest. This is the case until the cracks reach a length of 1.9 mm when fibre failures lead to fracture of the test piece in vacuum. Brisset [2] also found da/dN similar in vacuum at this temperature and in air at room temperature, finding the CA/CF for both to be the same.

Fracture surfaces and crack growth profiles display differences between tests in air and vacuum. It is evident from Fig. 9 that the tests performed in vacuum have on average much longer pull out lengths than tests performed in air (Fig. 7, Table 5). One of the main differences between the two are the position of these bridging fibres. It is clear from the images that there is limited pull out in the first few rows of fibres for the test performed in air, compared with the long pull out apparent in vacuum. These fibres will have been bridging the crack for a long time in vacuum, and therefore reducing the growth rates shown. These experiments need to be repeated with acoustic emission to identify more precisely when fibre failures occur. To date, deductions from sharp increases in da/dN are used to identify fibre failures.

Figure 10 displays fatigue crack growth data for all tests in vacuum at 450 °C. The initial ΔK_{app} ranged from 22 to 30 MPa \sqrt{m} . All tests initially have crack

Fig. 9 SEM images showing the pull out lengths of the test performed at 450 °C and an initial ΔK_{app} value of 30 MPa \sqrt{m}

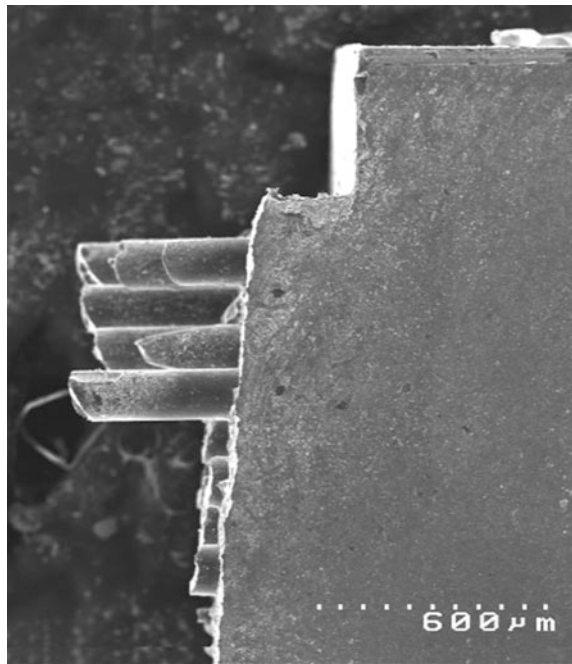


Table 5 Showing the average fibre pull out length and maximum pull out length measured from one side of the fracture face on a SEM for three tests

| Condition | Average pull out (mm) | S.D (mm) | Max pull out (mm) |
|--|-----------------------|----------|-------------------|
| 20 °C/AIR $\Delta K = 18 \text{ MPa}\sqrt{\text{m}}$ | 0.076 | 0.029 | 0.14 |
| 450 °C/AIR $\Delta K = 10 \text{ MPa}\sqrt{\text{m}}$ | 0.078 | 0.052 | 0.19 |
| 450 °C/VAC $\Delta K = 22 \text{ MPa}\sqrt{\text{m}}$ | 0.26 | 0.16 | 0.46 |

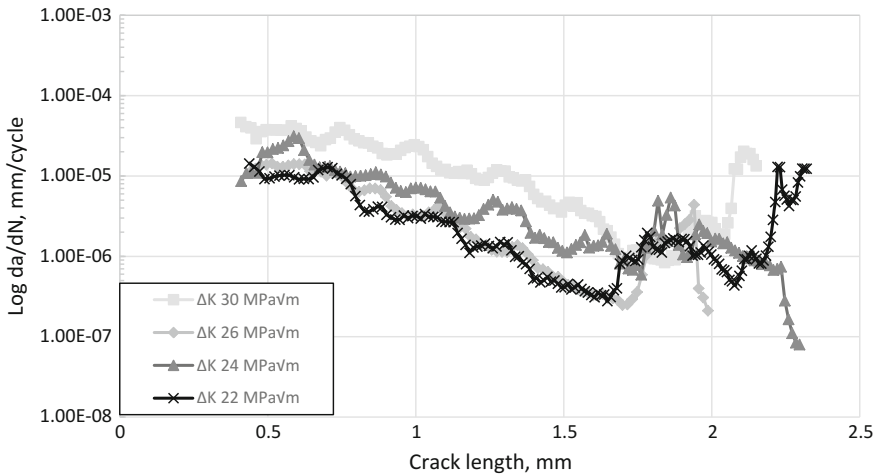


Fig. 10 Fatigue crack growth rate da/dN versus crack length for four different values of initial ΔK_{app} at $R = 0.1$ cycled at 4 Hz until failure or arrest at 450 °C in vacuum

growth rates scaled to the initial ΔK_{app} . All tests had very similar starting crack growth rates, but as the initial ΔK_{app} decreased, so too did the rate of growth. Even at the highest initial ΔK_{app} , crack growth rates decreased until final failure. All tests grew to a crack length of ~ 1.6 mm with decreasing crack growth rates. Figure 11 shows the effect of testing in vacuum, even at a higher test temperature, discussed earlier, and still has reduced da/dN compared to air. Earlier, the test temperature of 450 °C was found to have a reduced effect on the fatigue crack growth resistance of the composite. Taking this into account, Fig. 11 displays the benefits of vacuum. For the same initial ΔK_{app} , those tested in vacuum have higher resistance to fatigue cracks than those in air. This is due to the bridging fibres in the first few rows, which seem to bridge the crack for a very long time in vacuum.

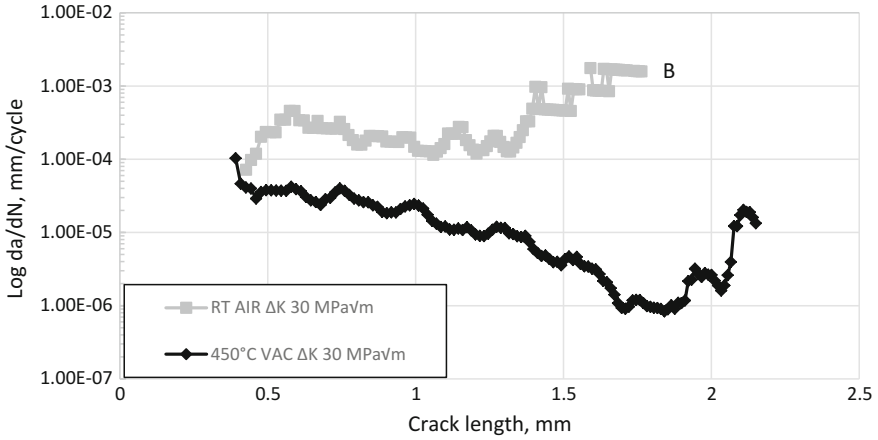


Fig. 11 Fatigue crack growth rate da/dN versus crack length for an initial ΔK_{app} $30 \text{ MPa}\sqrt{\text{m}}$ at room temperature in air and an ΔK_{app} $30 \text{ MPa}\sqrt{\text{m}}$ at 450°C in vacuum. *Note* The da/dN data for test that bifurcated is only displayed up to the bifurcation crack length

Effect of Stress Ratio, R , at Room Temperature and 450°C

Table 3 displays results from fatigue tests at stress ratios 0.5 and 0.7, both at room temperature and 450°C . At both temperatures, an increase in stress ratio decreases the stress intensity factor range at which crack arrest can occur. A CA/CF transition was not found at both R ratio values at 450°C as at initial ΔK_{app} values of 4 and $6 \text{ MPa}\sqrt{\text{m}}$ for 0.5 and 0.7 respectively, a fatigue crack did not initiate from the notch. At room temperature, the increase in stress ratio from 0.1 to 0.7 caused a decrease in the initial ΔK_{app} at which fatigue crack arrests. This trend agrees with the previous work by Brett et al. [5] and Cardona et al. [4].

The maximum applied stress intensity factor, K_{max} , after the crack has grown past the first row of fibres can also be used to quantify the CA/CF transition. This value, which is the same for all stress ratios at a given test temperature, should not be exceeded in order to keep the fibres intact and therefore to bridge the crack. Koval [13] found that at room temperature as the stress ratio increased, the K_{max} required for CA to occur increased. This suggests that the CA/CF transition is not only determined by K_{max} , but also by the initial ΔK_{app} .

Figure 12 displays fatigue crack growth data from tests performed at the same initial ΔK_{app} value ($10 \text{ MPa}\sqrt{\text{m}}$) for three R ratios (0.1, 0.5 and 0.7) [11]. Higher stress ratios decreases the resistance of the composite to fatigue crack growth. The only test to arrest was the one with a stress ratio of 0.1. As stated earlier, sharp excursions in da/dN are indicative of fibre failures. The two higher stress ratios promote increased fibre fracture.

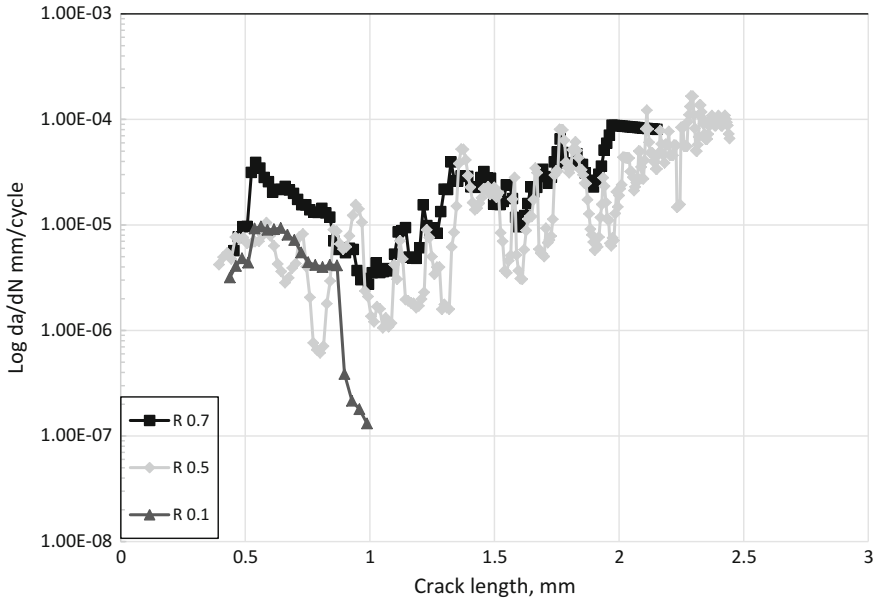


Fig. 12 Fatigue crack growth rate da/dN versus crack length for three different values of stress ratio, R , for tests in air at 450 °C. All tested at an initial ΔK_{app} of 10 $MPa\sqrt{m}$ and 4 Hz

Conclusions

The CA/CF transition is governed by the number of intact bridging fibre in the crack wake. A crack is deemed to have reached crack arrest if the growth rates fall below $da/dN \leq 10^{-8}$ mm/cycle. From the crack growth resistance curves it can be deduced that in tests which arrest few, if any, fibres have failed. Above this transition many fibres fail leading to the eventual fracture of the test piece.

At a given test temperature, initial ΔK_{app} determines the life of the composite. The higher the ΔK_{app} the more likely the test will fail. Bifurcation however, seems to be a function of test piece geometry and not affected by the initial loading conditions or test temperature.

There are modest effects of fatigue crack growth resistance between room temperature and 300 °C. Crack growth rates are very similar at a given crack length, up to 1.6 mm. Increasing the test temperature to 450 °C displays a much larger difference compared with room temperature. The CA/CF transition is greatly reduced at 450 °C, indicating temperature causes a change to the matrix resistance to fatigue cracks.

Testing in vacuum is advantageous compared with testing in air. Although a CA/CF transition is yet to be found, the fatigue crack growth data suggest this will be higher than in air at the same temperature. Individual fibre push out tests are required to assess the interfacial properties after tests in vacuum.

Fibre pull out lengths seem to be unaffected by an increase in temperature when observing test pieces that have arrested. The stark difference is observed in those tested in vacuum, where long pull out is observed in the first few rows of fibres, suggesting these rows are important in reducing crack growth rates.

An increase in stress ratio decreases the initial stress intensity factor range at which crack arrest can occur.

References

1. Cotterill P, Bowen P (1993) Fatigue crack growth in a fibre-reinforced titanium MMC at ambient and elevated temperatures. *Compos* 24(3):214–221
2. Brisset F, Bowen P (1998) Fatigue crack growth in fibre reinforced titanium MMC laminate at room and elevated temperatures. *Mater Sci Technol* 14(7):651–657
3. Bowen P (1996) Characterization of crack growth resistance under cyclic loading in the presence of an unbridged defect in fiber-reinforced titanium metal matrix composites. In: *Life prediction methodology for titanium matrix composites*. ASTM International
4. Cardona DC, Barney C, Bowen P (1996) Modeling and prediction of crack arrest in fiber-reinforced composites. In: *Life prediction methodology for titanium matrix composites*. ASTM International
5. Brett R, Cotterill P, Bowen P (1996) The influence of loading levels, temperature and environment on fibre failure during the fatigue of an SiC fibre reinforced Ti-MMC. *Int J Fatigue* 18(1):1–8
6. Doel T, Cardona D, Bowen P (1998) Fatigue crack growth in selectively reinforced titanium metal matrix composites. *Int J Fatigue* 20(1):35–50
7. Barney C, Cardona D, Bowen P (1998) Fatigue crack growth resistance from unbridged defects in continuous fibre reinforced metal matrix composites. *Int J Fatigue* 20(4):279–289
8. Ibbotson AR (1994) Fatigue crack growth in continuous fibre reinforced titanium alloy matrix composites. University of Birmingham
9. Dear MN (2016) Fatigue in SiC fibre reinforced titanium metal matrix composites. University of Birmingham
10. Zamperini S (2002) Effects of cyclic loading on fibre reinforced titanium metal matrix composites. University of Birmingham
11. Grantham-Wright H (2017) Fatigue crack growth resistance in fibre-reinforced titanium metal matrix composites. University of Birmingham
12. Liu J, Bowen P (1999) Bridging mechanisms in fibre-reinforced Ti MMCs. *ROLLS ROYCE PLC-REPORT-PNR*
13. Koval O (2016) Fatigue in SiC fibre reinforced titanium metal matrix composites. University of Birmingham